ARCHIVES OF ACOUSTICS
23, 2, 291–305 (1998)

FINITE ELEMENT METHOD (FEM) AND IMPULSE RESPONSE METHOD (IRM) ANALYSIS OF CIRCULAR ULTRASONIC TRANSDUCERS

P. KIEŁCZYŃSKI

Section of Acoustoelectronics
Institute of Fundamental Technological Research,
Polish Academy of Sciences
(00-049 Warsaw, Świętokrzyska 21, Poland)

Circular transducers with axially-symmetric vibrational profiles were considered. Vibrational patterns of transducer structures were calculated using the Finite Element Method. Analytical formulas for the impulse response function $h(X,t)$ for circular transducers and vibration velocity profiles, approximated by linear and quadratic polynomials, on the finite element (annulus) were established. These formulas enable accurate calculations of acoustic field distributions in near and far-field, respectively. Calculated profiles of an acoustic field were compared with the experimental data.

1. Introduction

Ultrasonic transducers employed in robotics, non-destructive testing (NDT) and acoustic imaging often have compound structures and circular symmetry. The vibrational patterns of ultrasonic transducers which exist in reality are non-homogeneous and only in a simplified analysis can those profiles be treated as constant ones.

The objective of this paper is to analyze the performance of circular ultrasonic transducers having a non-homogeneous distribution of the vibrational velocity (normal particle velocity) on their surface. The profiles of the vibration distribution on the transducer surface determine the properties of radiation patterns in the near and far zones, respectively. This is why producing proper vibrational profiles is an essential factor in the process of analysis and synthesis (developing) of ultrasonic transducers of given directivity patterns.

The first method used for calculating the distribution of the acoustic field was the Kirchhoff Integral Method. This is a direct and natural method which in general gives reliable results. However, this method has its limitations and is not fully justified mathematically.

Among other methods of calculating the acoustic field distribution, let us mention the Green Function Method [1], Integral Equation Method [2], Finite Element Method (FEM) [3–7], Boundary Element Method (BEM) [8, 9], Variational Methods [10] etc. In all those methods (except BEM) two-dimensional integrals must be evaluated. It is

laborious and time consuming. By applying the BEM, the dimension of the problem is reduced by one. On the other hand, the matrices obtained using the BEM are full and non-symmetric.

A considerable simplification in the calculations of the acoustic field distribution can be achieved when the Rayleigh–Helmholtz (Kirchhoff) integral is presented as a convolution of two functions of time. This constitutes a basis of the Impulse Response Method (IRM) of determining the acoustic field distribution.

The acoustic field distribution in the near and far zones was evaluated using the Impulse Response Method [11–22]. Acoustic field distributions calculated by this method are exact and are obtained without applying the Fresnel or Fraunhofer approximations. Moreover, in the IRM only one dimensional integrations are performed. By contrast, in the classical Kirchhoff Integral Method two-dimensional integrals must be calculated [23, 24].

In this paper, the impulse response function $h(X,t)$ was established for circular transducers and the vibrational velocity profiles approximated by linear and quadratic polynomials of the variable ϱ (along the transducer radius) on the finite element (annulus). Those profiles can result from the application of the FEM in the analysis of the transducer's vibrations.

Mechanical vibrations of the transducer structure are governed by a system of differential equations of motion along with the appropriate boundary conditions. In this way the eigen problem (Sturm–Liouville problem) is determined. The eigenvector corresponds to the vibrational pattern and the eigenvalue is proportional to the eigen frequency of the structure. The transducer structure has an axial symmetry, thus, the vibrational velocity vector has two components (v_z, v_ϱ), where v_z is a vertical component along the z axis, and v_ϱ is a radial component along the radius ϱ of the transducer.

One of the most frequently used approximate methods is the Finite Element Method (FEM). After applying the FEM, the initial differential problem is transformed into a matrix problem. Once the problem has been solved, we obtain a spatial distribution of the approximate eigenvector (v_z, v_ϱ). The transducer structure is divided into a set of finite elements. At a finite numbers of nodes, the eigenvector has exact values (interpolation). At other points of the transducer structure, the eigenvector is approximated by using the polynomials of z and ϱ. On the transducer surface ($z = \text{const}$), we have: $v_z = v_z(\varrho)$. The vertical component of the vibration velocity v_z is the source of an acoustic field outside the transducer.

In the case of harmonic excitation of pulsation ω_0, the time dependence of a vibrational velocity is a follows:

$$v(t) = v_0 \exp(j\omega_0 t). \tag{1}$$

The acoustic pressure at an observation point X is given by [15]:

$$p(X,t) = j\omega_0 \varrho_m h(X,t)^* v(t), \tag{2}$$

where: $*$ denotes a convolution operator, ϱ_m is the density of the medium.

The impulse response function $h(X,t)$ depends both on the transducer geometry and on the distribution of the vibrational velocity on the transducer surface. The radiating transducer face is planar and is placed in the infinite rigid baffle.

Equation (2) can be written in the form:

$$p(X,t) = j\omega_0 \varrho_m v_0 \exp(j\omega_0 t) \int_{-\infty}^{+\infty} h(X,\tau) \exp(-j\omega_0 \tau)\, d\tau. \tag{3}$$

As it is seen from Eq. (3), to calculate the value of the acoustic pressure at point X, the Fourier transform of the impulse response function $h(X,t)$ (treated as a function of time) must be evaluated. In the paper, a description of the construction of manufactured ultrasonic transducers is presented. Also, an experimental set-up for measuring the acoustic field distribution generated by the considered circular transducers was described. The results of numerical calculations (Eq. (7)) were compared with experimentally measured distributions of the acoustic field.

2. Methods of calculation of the vibrational velocity profiles of ultrasonic transducers

Exact analytical formulas for vibrational velocity profiles are known only in the case of transducers with simple geometry. This is why for real transducer structures approximative methods should be used to evaluate vibrational profiles [25–31].

Among them one can distinguish variational methods, which were applied by EER NISSE and HOLLAND [32, 33] for the analysis of circular ultrasonic transducers.

Until now, the most popular numerical method was the Finite Difference Method [34]. However, applying this method in the case of complex mechanical structures (composites) was tedious. The FEM and BEM belong to the most exact and mathematically justified methods. The FEM was applied to analyze the performance of ultrasonic transducers in papers [35–41].

In the finite element approximation of axisymmetric solids, the continuous structure is replaced by a system of axisymmetric elements, e.g. for a glass cylinder the finite element is a hollow cylinder (rectangular torus). The intersections of those elements with an upper surface of the glass cylinder decomposes that surface into a set of annuli which are treated in the two-dimensional analysis as finite elements (see Fig. 1).

The vibrational velocity $v = (v_z, v_\varrho)$ on the upper surface ($z = \text{const}$) of the cylinder is a function of the radius ϱ. On each finite element (annulus), the velocity profile can be approximated by polynomials of finite order of the variable ϱ, e.g. for the linear approximation and a vertical component of the vibrational velocity v_z we have:

$$v_z(\varrho) = a_0 + a_1 \varrho, \tag{4}$$

where: the coefficients a_0 and a_1 are given from FEM calculations, ϱ corresponds to the variable along the transducer radius, the coefficient a_0 describes a constant velocity profile.

In this paper, analytical formulas for the impulse response function $h(X,t)$ generated by the profile (4) were established. Then, employing the IRM the theoretical profiles of an acoustic field in the near and far zones were calculated.

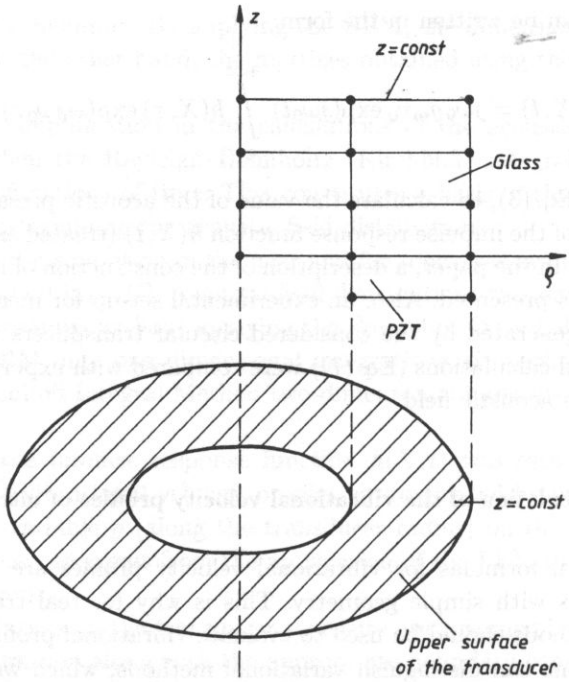

Fig. 1. Schematic view of the finite element model of the axisymmetric transducer structure. The set of two rings represents the upper surface of the transducer.

3. Acoustic field distributions resulting from the application of FEM in calculations of vibrational velocity profiles

For the linear profiles Eq. (4) the analytical formulas for the impulse response function were established by the author. Those formulas make it possible to calculate the acoustic field distribution generated by each annulus. The total acoustic field is obtained by summing the components originated by each individual annulus. For the constant velocity profile, $v_z(\varrho) = 1$, we have:

$$h_0(X,t) = c/2\pi(\theta_2 - \theta_1). \tag{5}$$

For the linear profile $v_z(\varrho) = \varrho$, the impulse response function is the following one:

$$h_1(X,t) = c/2\pi\sqrt{u^2+r^2}\sum_{n=0}^{\infty}\binom{1/2}{n}(-1)^n k^n \int_{\theta_1}^{\theta_2}\cos^n\theta\, d\theta, \qquad 0 \le k < 1,$$

$$h_1(X,t) = \frac{-2c}{\pi}u\left(\cos\frac{\theta_2}{2} - \cos\frac{\theta_1}{2}\right), \qquad k = 1, \tag{6}$$

$$h_1(X,t) = cu, \qquad k = 0,$$

where:

$$k = \sqrt{\frac{2ur}{u^2+r^2}}, \qquad c \text{ is the sound velocity in the medium.}$$

The symbols u, r, X and from Eqs. (4)–(6) are marked in Fig. 2.

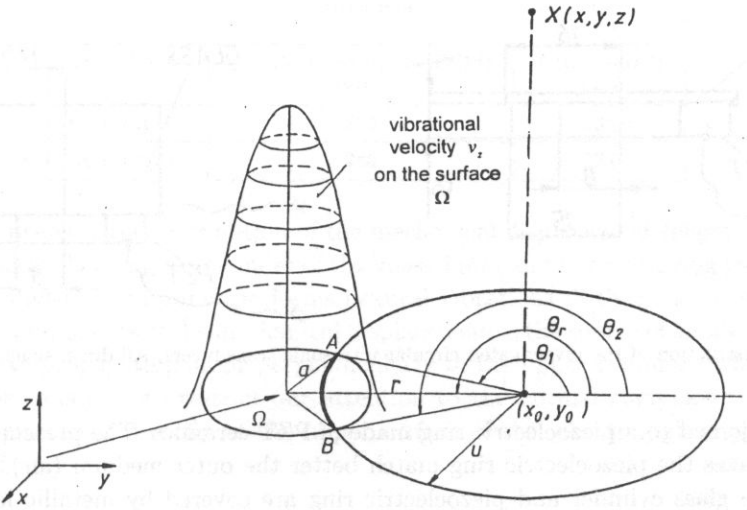

Fig. 2. Geometry of the problem for circular transducers. The integral is calculated along the arc AB. a is the transducer radius, Ω is the transducer surface.

The impulse response function for the profile (4) is as follows:

$$h(X,t) = a_0 h_0(X,t) + a_1 h_1(X,t). \tag{7}$$

Formula (7) was used in the calculations of acoustic fields in the near and far zones, respectively. For circular transducers and a quadratic approximation of vibrational velocity profiles, e.g. $v_z(\varrho) = \varrho^2$, we have

$$h(X,t) = \left[(u^2 + r^2)(\theta_2 - \theta_1) - 2ur(\sin\theta_2 - \sin\theta_1)\right]. \tag{8}$$

Equation (8) together with Eq. (7) can be used to calculate the acoustic field distribution resulting from the application of the approximation of the vibrational velocity (on each element) by polynomials of first and second order.

4. Examples of transducer constructions

The majority of ultrasonic transducers used in robotics have a circular symmetry and layered structure. For instance, the elastic waveguide (cylinder) is stimulated to vibrations by a piezoelectric element (ring). Ultrasonic transducers of the Langevin type applied in echolocation and non-desctructive testing display also a similar construction.

Bearing in mind the suggestions mentioned, we constructed ultrasonic circular transducers at the Acoustoelectronics Section of the Institute of Fundamental Technological Research (see Fig. 3a, b). The symmetry axis of the circular transducers is depicted by a broken line. The vibrating elastic (glass) cylinder is a source of acoustic waves propagating in the outer medium (air) perpendicularly to the upper cylinder surface. This

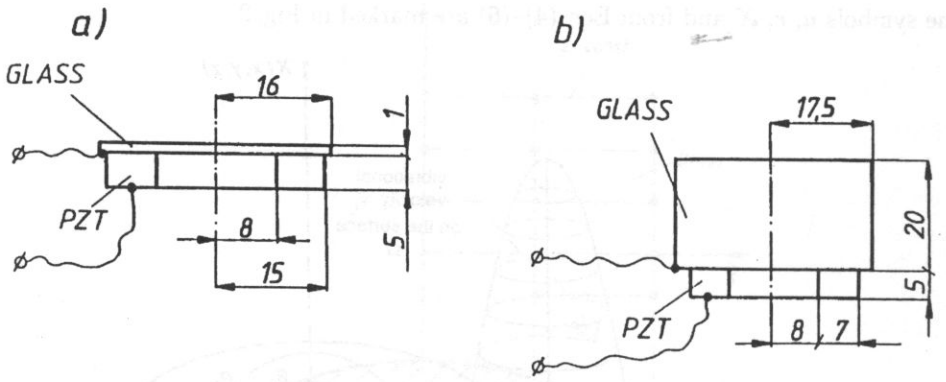

Fig. 3. Construction of the investigated circular ultrasonic transducers. All dimensions are in mm.

cylinder is joined to a piezoelectric ring made of PZT ceramics. The presence of a glass cylinder makes the piezoelectric ring match better the outer medium (air). Lower surfaces of the glass cylinder and piezoelectric ring are covered by metallic layers which constitute electrodes driven by an alternating electric voltage.

Glass cylinders of small thickness (1 mm) can be treated as membranes performing flexural vibrations. Thicker cylinders (10 mm) vibrate in a more complicated way. Depending on the thickness to diameter ratio, the cylinder can vibrate in thickness, radial or extensional modes. The applied electric voltage excites the piezoelectric ring into vibrations perpendicularly to the electrode surfaces.

4.1. Numerical analysis of transducer vibrations

Numerical calculations of the eigen-frequencies were performed for ultrasonic transducers composed of a ceramic ring and glass cylinder. To this end, a computer program ANSYS implemented on an IBM-PC computer was used. This program calculates (by using the FEM) distributions of the mechanical displacement and stresses in the mechanical system analyzed.

The numerical experiment was carried out and enabled an assessment of the eigenfrequencies (eigenvalues) and 3-dimensional vibrational patterns (eigenvectors) of the considered ultrasonic transducers. The material parameters used in the calculations are presented in Table 1. The measured values of the resonant frequencies of the vibrating transducers are shown in Table 2. This table also contains the values of corresponding eigenfrequencies calculated numerically.

Table 1. Material parameters of transducer structures.

Material	Young Modulus N/m^2	Density kg/m^3
PZT Ceramics	7.1E + 10	7.5E + 3
Glass	7.5E + 10	2.6E + 3

Table 2. Measured and calculated (by the FEM) values of resonant frequencies of the transducer structures.

Transducer	f (calculated by the FEM) [kHz]	f (measured) [kHz]
from Fig. 3a	238	234
from Fig. 3b	245	234

Figure 4 presents the distribution of the mechanical displacement (eigen-vector) calculated numerically of a glass cylinder of thickness 1 mm and a ceramic ring (see Fig. 3a). The glass cylinder (membrane) performs flexural vibrations (9-th mode, $f = 238\,\text{kHz}$). The normal components of the mechanical displacement is the source of an ultrasonic longitudinal wave propagating in air perpendicularly to the upper cylinder surface. Hence, in the further analysis we restrict our attention to the normal component of the mechanical displacement directly at the upper surface of the vibrating glass cylinder, see Figs. 4 and 5.

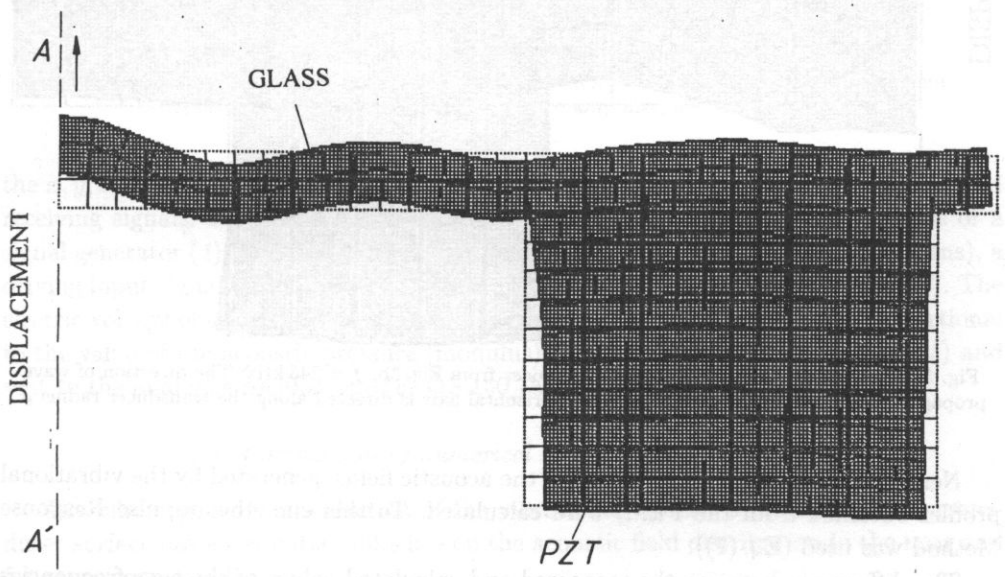

Fig. 4. Distribution of the mechanical displacement of vibrating transducer from Fig. 3a. The axis AA' is a symmetry axis of the transducer, $f = 238\,\text{kHz}$. The direction of wave propagation (along the z axis) is marked by arrow.

In Fig. 4, one half of the ultrasonic transducer from Fig. 3a is presented. A complete structure of the transducer is obtained by rotating the structure from Fig. 4 along the symmetry axis AA'. Figure 4 displays the real proportions of the analysed transducer from Fig. 3a. Figure 5 presents (analogously to Fig. 4) a distribution of the mechanical displacement of the transducer from Fig. 3b. The distribution of the vibrational amplitude (eigenvector) is seen in the dark part of Fig. 5, while the rectangular grid, visible in the background, represents the transducer structure at rest.

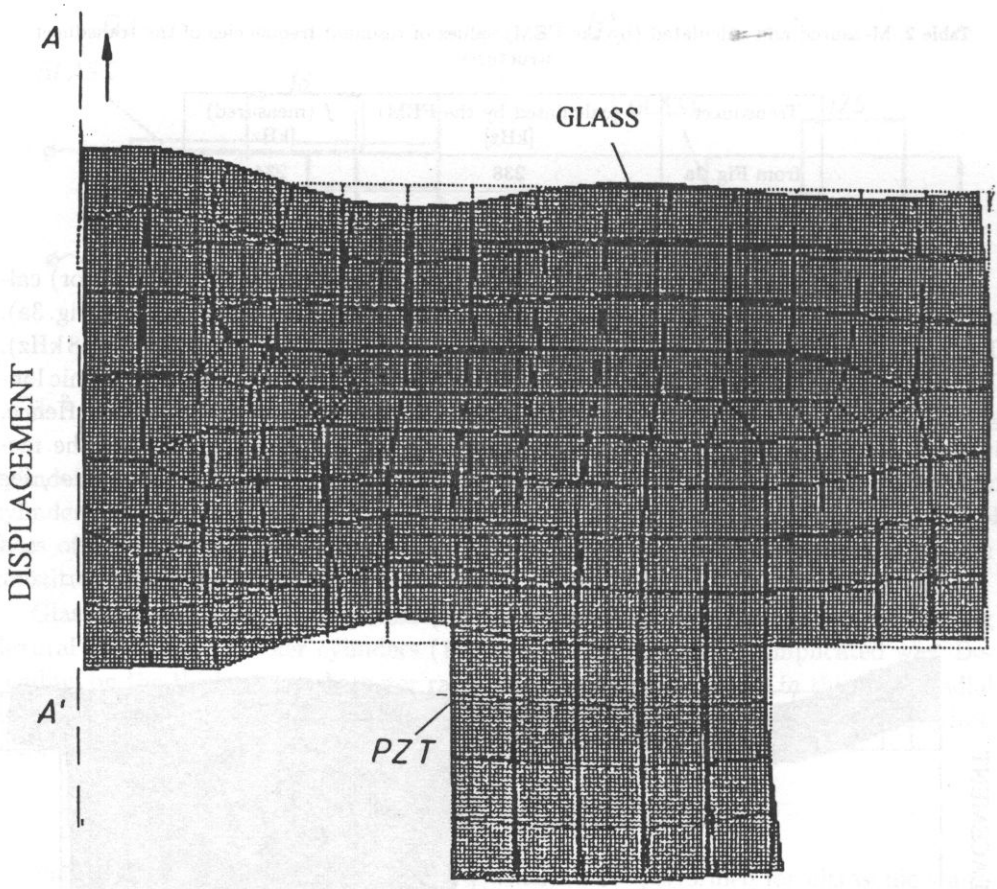

Fig. 5. Eigen-vibration pattern of the transducer from Fig. 3b. $f = 245$ kHz. The direction of wave propagation is indicated by an arrow. The horizontal axis is directed along the transducer radius ϱ.

Next, the theoretical distributions of the acoustic fields, generated by the vibrational profiles obtained from the FEM, were calculated. To this end, the Impulse Response Method was used (Eq. (7)).

The differences between the measured and calculated values of the eigenfrequencies (see Table 2) can be explained by the discrepancy of the real and assumed values of the material parameters.

4.2. Description of experimental set-up

Experimental investigations of circular ultrasonic transducers were performed in the measuring laboratory set-up [42, 43], see Fig. 6. The laboratory set-up contained mechanical components, the investigated the ultrasonic transducers and electronic apparatus. The measured transducers (*3*) were fixed. The moving part of the laboratory set-up consisted of a measuring probe (*4*) fixed in a special holder providing translation along

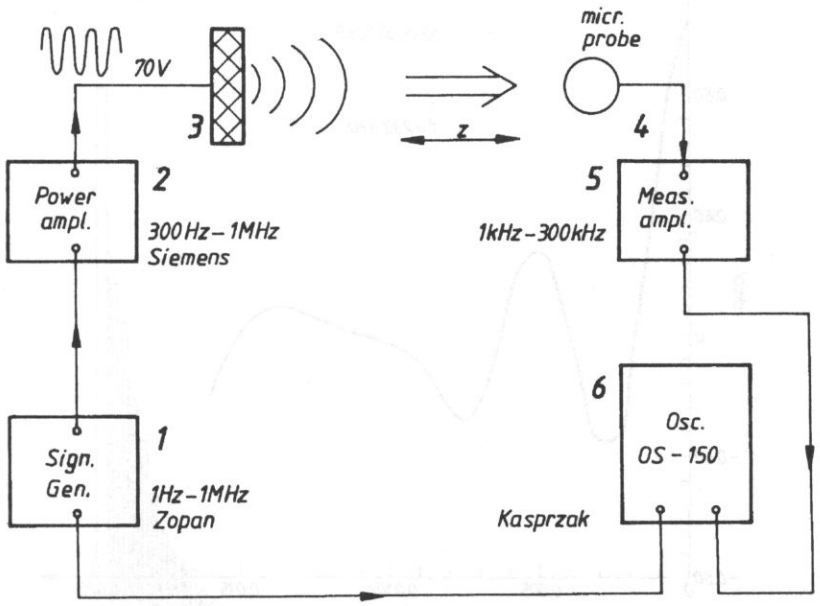

Fig. 6. Laboratory measuring set-up. *1* – signal generator, *2* – power amplifier, *3* – ultrasonic transducer, *4* – probe (microphone), *5* – amplifier, *6* – oscilloscope.

the x, y, z axes. The electronic part of the set-up constituted devices for generating and receiving signals. The investigated transducer was excited to vibration by means of a signal generator (*1*) (Zopan). After being amplified in a power amplifier (*2*) (Siemens), a driving input signal of amplitude 70 V was applied to the transducer electrodes (*3*). The electric voltage obtained from a miniature piezoelectric microphone (*4*) was proportional to the value of the acoustic pressure (modulus). Then this signal was amplified (*5*) and sent to the analogue oscilloscope (*6*) OS-150 (Kasprzak).

4.3. Comparison of numerical and experimental results

The inhomogeneous distribution of the vibrational velocity amplitude on the transducer surface has an essential influence on the acoustic field distribution in the near and far zones respectively.

Measurements of the acoustic field distribution generated by the ultrasonic transducers constructed (see Fig. 3a, b) were carried out.

In reality, vibrating structures are more complicated than those of the theoretical considerations. The range of the theoretical beam is greater than that in the experiment. This fact can be explained by attenuation in the real experimental environment.

The ranges of the theoretical and experimental beams were determined from the curves representing changes of the acoustic pressure along the z axis. A decline of the acoustic pressure from its maximum value $|p_{\max}|$ to the level $0.7|p_{\max}|$ on the monotonically descending part of the curve defines the range of the considered acoustic beam, where $|p_{\max}|$ is the maximum value of the last oscillation.

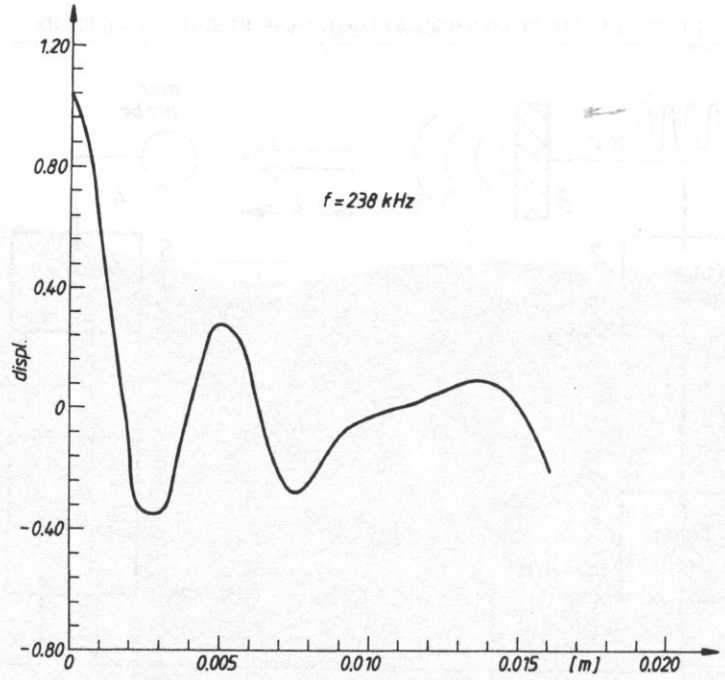

Fig. 7. Distribution (calculated by the FEM) of the z component of the mechanical displacement on the surface of the circular transducer from Fig. 3a.

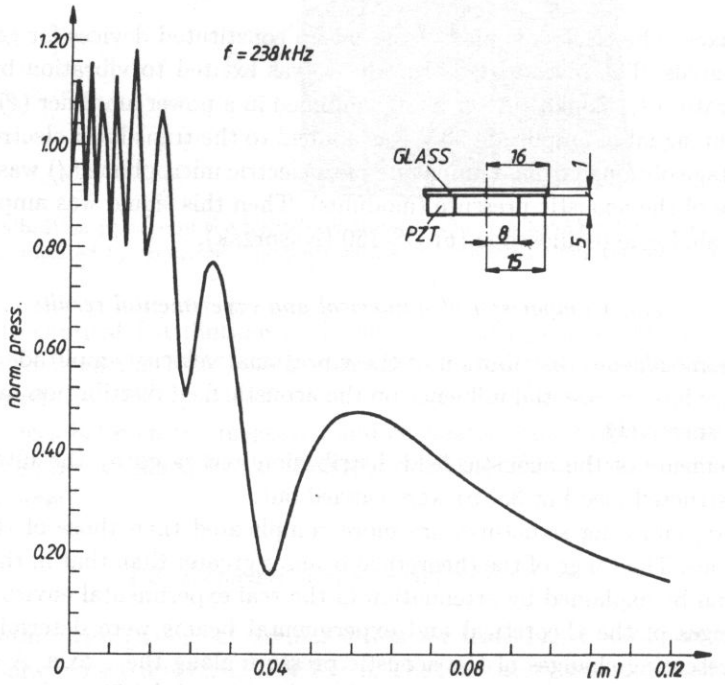

Fig. 8. Acoustic pressure distribution (calculated by the IRM) along the z axis of the transducer from Fig. 3a, generated by the distribution from Fig. 7.

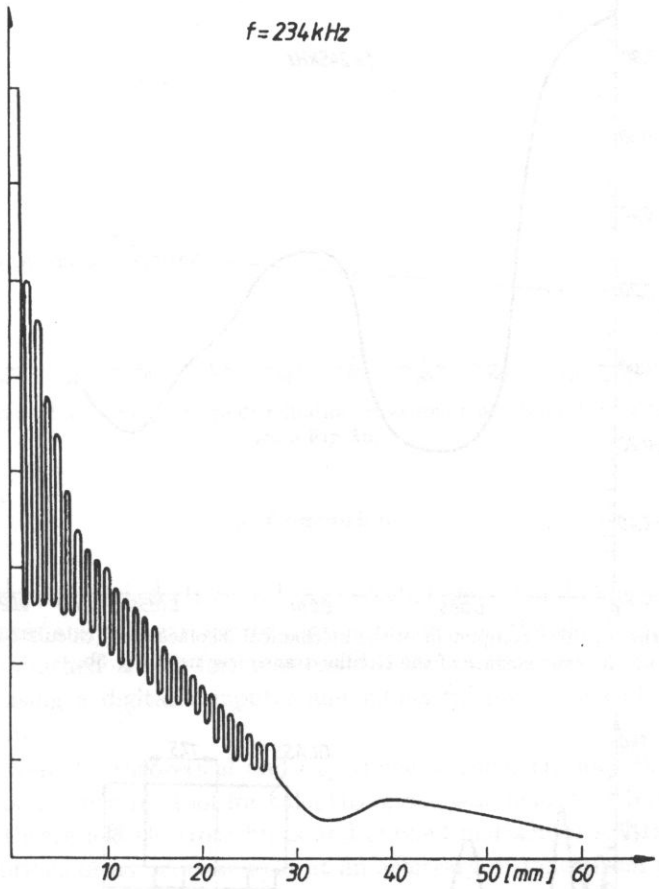

Fig. 9. Experimental acoustic pressure distribution measured along the z axis of the transducer from Fig. 3a.

Figures 7, 8 and 9 correspond to the ultrasonic transducer from Fig. 3a. Figure 7 describes the mechanical displacement distribution calculated by the FEM in the direction perpendicular to the upper surface of the glass cylinder (plate). Figure 8 represents the acoustic field distribution, calculated by the IRM, on the z axis outside the transducer. In Fig. 9 the acoustic field distribution measured along the z axis is plotted. Comparing Figs. 8 and 9 one can state that the range of the theoretical beam from Fig. 8 equals 8 cm and is greater than the measured range (5 cm), see Fig. 9.

Figures 10, 11 and 12 correspond analogously to the ultrasonic transducer from Fig. 3b. It is apparent that the theoretical range from Fig. 11 equals 10 cm and is greater than that of the experimental beam (6 cm) from Fig. 12.

Measurements of the acoustic pressure along the z axis were carried out at points being 1 mm away from each other. In the interference zone, the distance between the measuring points was 0.5 mm. In numerical calculations and experiments, the absolute values (moduli) of the acoustic pressure were measured and evaluated.

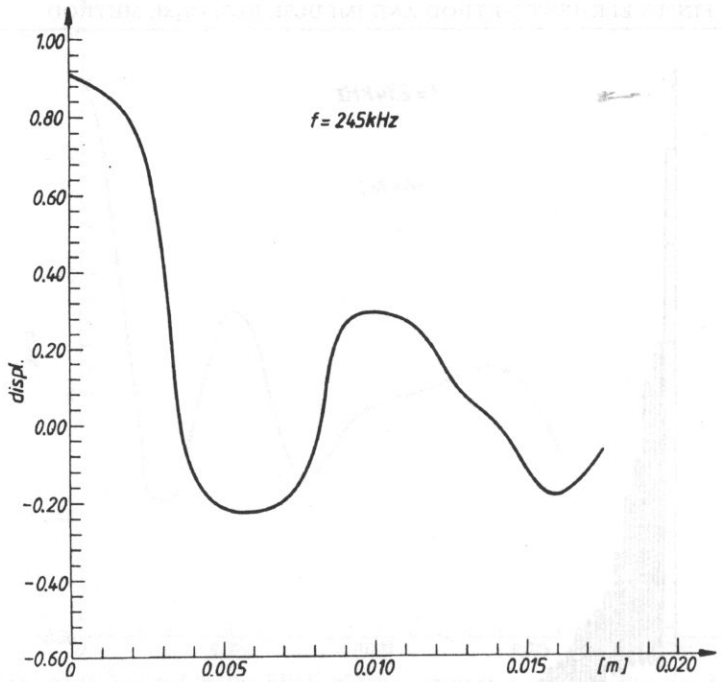

Fig. 10. Distribution of the z component of the mechanical displacement (calculated by the FEM) on the surface of the circular transducer from Fig. 3b.

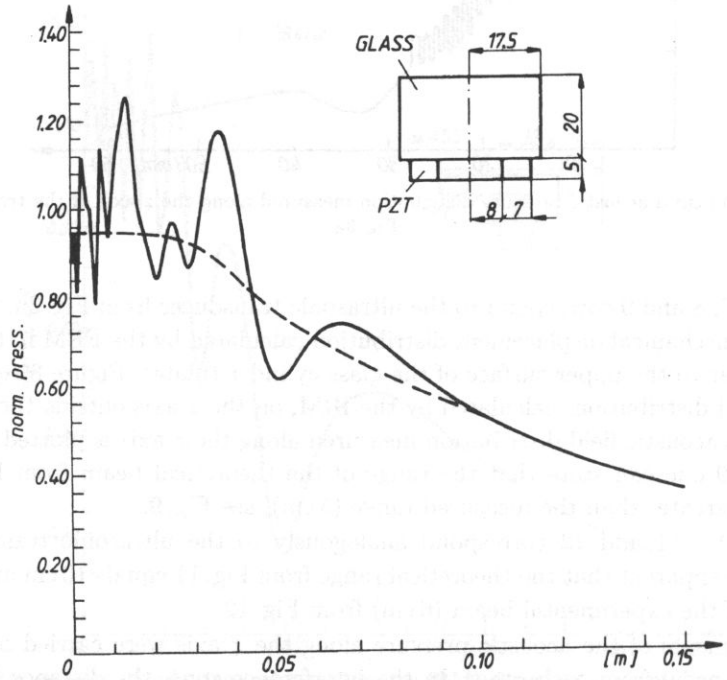

Fig. 11. Acoustic pressure distribution (calculated by the IRM) along the z axis of the transducer from Fig. 3b, generated by the distribution from Fig. 10. The broken line represents the mean value of the calculated acoustic pressure modulus.

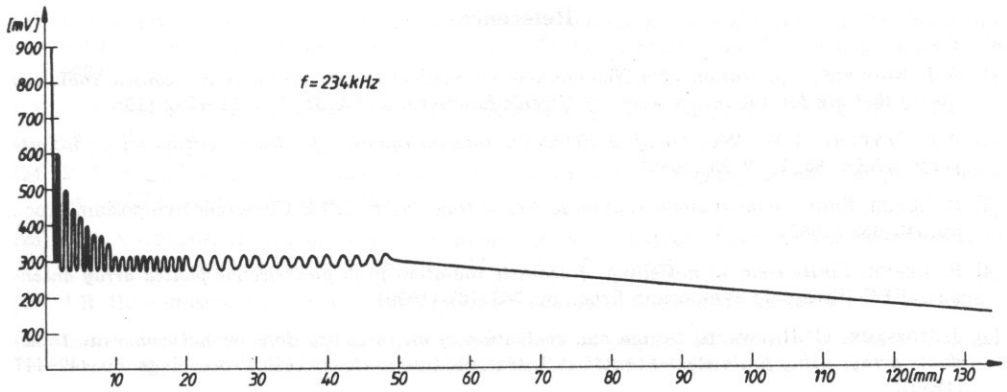

Fig. 12. Experimental acoustic pressure distribution measured along the z axis of the transducer from Fig. 3b.

5. Conclusions

The analytical formulas for the impulse response function $h(X,t)$ in the case of circular transducers and a linear approximation of the vibrational velocity on the finite element were established. Those formulas enabled the calculations of the acoustic field distribution by using a digital computer and numerical procedures of evaluating the Fourier transform.

As resulted from the theoretical and experimental considerations the Impulse Response Method is an effective tool for calculating acoustic field distributions based on the concepts of theoretical electrotechnics and applied mathematics. It makes possible the exact calculations of an acoustic field at an arbitrary distance from the transducer surface.

The application of other mathematical methods, e.g. the Boundary Element Method [8], can also be useful, for instance, in the calculations of non-stationary acoustic field distributions. This method (BEM) may be applied also for the general problem, i.e. in the case when the vibrational pattern of the transducer and the resulting acoustic field distribution in the outer medium are analysed and calculated simultaneously.

The performed numerical calculations and experiments confirmed the validity of the established analytical formulas as well as the proposed method of analyzing ultrasonic transducers.

By applying the FEM, various combinations of materials and their parameters can be taken into account. Applying the IRM, quick and accurate calculations of the radiation characteristics of the considered ultrasonic transducer are possible.

The interface between the results of calculations resulting from the FEM and IRM was established. In this way an efficient software tool for the modelling and designing of ultrasonic transducers was constructed. This is of great importance in the development of ultrasonic composite transducers of a given directivity pattern and frequency characteristics.

References

[1] A.J. RUDGERS, *Application of a Neumann-series method to two problems in acoustic radiation theory that are formulated in terms of Green's functions*, JASA, **79**, 5, 1211–1222 (1986).

[2] A.F. SEYBERT, T.W. WU, *Modified Helmholtz integral equation for bodies sitting on an infinite plane*, JASA, **85**, 1, 19–23 (1989).

[3] R. LERCH, *Finite element analysis of piezoelectric transducers*, IEEE Ultrasonic Symposium Proc., pp. 643–653 (1988).

[4] R. LERCH, *Finite element modelling of acoustic radiation from piezoelectric phased array antennas*, IEEE Ultrasonic Symposium Proc., pp. 763–767 (1990).

[5] J. HOSSACK, G. HAYWARD, *Design and evaluation of one and two dimensional composite transducer arrays using finite element method*, Ultrasonic International 1989 Proceedings, pp. 442–447 (1989).

[6] K.W. COMMANDER, R.J. MCDONALD, *Finite element solution of the inverse problem in bubble swarm acoustics*, JASA, **89**, 2, 592–597 (1991).

[7] HIROFUMI OKADA, MINORU KUROSAWA, SADAYUKI UEHA, MICHIYUKI MASUDA, *New airborne ultrasonic transducer with high output sound pressure level*, Japanese Journal of Applied Physics, **33**, Part 1, 5B, 3040–3044 (1994).

[8] R.D. CISKOWSKI, C.A. BREBBIA, *Boundary Methods in Acoustics*, Elsevier, London 1991.

[9] R. LERCH, H. LANDERS, W. FRIEDRICH, R. HEBEL, A. HOS, H. KAARMANN, *Modelling of acoustic antennas with a combined finite-element-boundary-element-method*, IEEE 1992, Ultrasonic Symposium Proc., pp. 581–584 (1992).

[10] A.D. PIERCE, *Variational formulations in acoustic radiation and scattering*, [in:] Physical Acoustics Vol. XXII, THUSTON and PIERCE [Eds.], Academic Press, Boston 1993, pp. 195–371.

[11] P.R. STEPANISHEN, *Transient radiations from pistons in an infinite planar baffle*, JASA, **49**, 5 (Part 2), 1629–1638 (1971).

[12] J.C. LOOKWOOD, J.G. WILLETE, *High-speed method for computing the exact solution for the pressure variations in the nearfield of a baffled piston*, JASA, **53**, 3, 735–741 (1973).

[13] A. PENTTINEN, M. LUUKKALA, *The impulse response and pressure nearfield of a curved ultrasonic radiator*, J. Phys. D: Appl. Phys., **9**, 10, 1547–1557 (1976).

[14] HARRIS, *Review of transient field theory for a baffled planar piston*, JASA, **70**, 1, 10–20 (1981).

[15] J.NAZE TJOTTA, S. TJOTTA, *Nearfield and farfield of pulsed acoustic radiators*, JASA, **7**, 4, 824–834 (1982).

[16] S. KRENK, *Geometrical aspects of acoustic radiation from a shallow spherical cap*, JASA, **74**, 5, 1617–1622 (1983).

[17] W.A. VERHOEF, M.J.T.M. CLOOSTERMANS, J.M. THIJSSEN, *The impulse response of a focused source with an arbitrary axisymmetric surface velocity distribution*, JASA, **75**, 6, 1716–1721 (1984).

[18] H. LASOTA, R. SALOMON AND B. DELANNOY, *Acoustic diffraction analysis by the impulse response method: A line impulse response approach*, JASA, **76**, 1, 280–290 (1984).

[19] H. LASOTA, *Diffraction of acoustic plane wave: A time domain analysis*, JASA, **78**, 3, 1086–1092 (1985).

[20] L.GOMEZ ULARTE, J.L SAN EMETERIO PRIETO, *On The Impulse Response Of Rectangular Baffled Pistons*, Ultrasonic International, Conference Proceedings, pp. 566–571, 1989.

[21] F.M.J. LINSEN, A.F.G. HOEKS, *Transducer characterisation from pressure amplitude distribution measurements using a Kalman filter as parameter estimation algorithm*, Ultrasonic Imaging, **12**, 309–323 (1990).

[22] B. PIWAKOWSKI, K. SBAI, B. DELANNOY, *Computer-aided computing of acoustic field radiated from arbitrarily structured transducer arrays*, IEEE Ultrasonic Symposium Proceedings, pp. 983–986, 1994.

[23] J. ZEMANEK, *Beam behavior within the nearfield of a vibrating piston*, JASA, **49**, 1 (Part 2), 181–191 (1971).

[24] E.G. WILLIAMS, J.D. MAYNARD, *Numerical evaluation of the Rayleigh integral for planar radiators*, JASA, **72**, 6, 2020–2030 (1982).

[25] K.P. SOLDATOS, *Review of three dimensional dynamic analyses of circular cylinders and cylindrical shells*, Applied Mechanics Review, **47**, 10, 501–516 (1994).

[26] J.R. HUTCHINSON, *Vibrations of solid cylinders*, Journal of Applied Mechanics, **47**, 901–907 (1980).

[27] O.G. GUSTAFSSON, T.R. KANE, *Axially symmetric extensional vibrations of a circular disk with a concentric hole*, Journal of Applied Mechanics, **26**, 541–545 (1959).

[28] J.R. HUTCHINSON, *Axisymmetric vibrations of a free finite-length rod*, JASA, **51**, 1 (Part 2), 233–240 (1972).

[29] A. IULA, N. LAMBERTI, M. PAPPALARDO, *A matrix model of the thin piezo-electric ring*, IEEE Ultrasonic Symposium Proc., pp. 921–924, 1994.

[30] J. ZEMANEK, *An experimental and theoretical investigation of elastic wave propagation in a cylinder*, JASA, **51**, 1 (Part 2), 265–283 (1972).

[31] M. BRISSAUD, *Three-dimensional modelling for ring and tube piezoceramics*, Ultrasonics International Conference Proceedings, pp. 647–652, 1989.

[32] E.P. EERNISSE, *Varational method for electroelastic vibration analysis*, IEEE Trans. on Sonics & Ultrasonics, **SU-14**, 153–160 (1967).

[33] R. HOLLAND, E.P. EERNISSE, *Variational evaluation of admittances of multielectroded three-dimensional piezoelectric structures*, IEEE Trans. on Sonics & Ultrasonics, **SU-15**, 2, 119–132 (1968).

[34] G.W. MCMAHON, *Finite difference analysis of the vibrations of solid cylinders*, JASA, **48**, 1 (Part 2), pp. 308–312 (1969).

[35] H.A. KUNKEL, S. LOCKE, B. PINKERTON, *Finite element analysis of vibrational modes in piezoelectric ceramic disk*, IEEE Trans. on UFFC, **37**, 4, 316–328 (1990).

[36] R. LERCH, *Simulation of piezoelectric devices by two and three-dimensional finite elements*, IEEE, Ultrasonic Symposium Proc., pp. 233–247 (1990).

[37] P. CHALLANDE, *Optimizing ultrasonic transducers based on piezoelectric composites using a finite element method*, IEEE Trans. on UFFC, **37**, 3, pp. 135–140 (1990).

[38] R.W. CLOUGH, F. ASCE, Y. RASHID, *Finite element analysis of axisymmetric solids*, Journal of the Engineering Mechanics Division, pp. 71–85 (1965).

[39] JUN LAN, M.J. SIMONEAU, R.K. JEFFREYS, S.G. BOUCHER, *A complete finite element model*, IEEE, Ultrasonic Symposium Proceedings, pp. 999–1003 (1994).

[40] J.T. STEWART, *Finite element modeling of resonant microelectro-mechanical structures for sensing applications*, IEEE, Ultrasonic Symposium Proc., pp. 643–646 (1994).

[41] P. KIEŁCZYŃSKI, W. PAJEWSKI, M. SZALEWSKI, *Finite Element Method (FEM) and Impulse Response Method (IRM) analysis of circular and rectangular transducers*, IEEE Ultrasonic Symposium in Seattle (USA), 1995.

[42] W. PAJEWSKI, M. SZALEWSKI, *Piezoelektryczne przetworniki ultradźwiękowe promieniujące do powietrza*, Prace IPPT, 4/1992.

[43] W. PAJEWSKI, P. KIEŁCZYŃSKI, M. SZALEWSKI, *Radiations of piezoelectric rings into the air through cylindrical waveguides*, Archives of Acoustics, **20**, 4, 361–372 (1995).